

# Stability of hydrogenation states of graphene and conditions for hydrogen spillover

Sang Soo Han,<sup>1</sup> Hyun Jung,<sup>2</sup> Dong Hyun Jung,<sup>3,\*</sup> Seung-Hoon Choi,<sup>3</sup> and Noejung Park<sup>2,†</sup><sup>1</sup>*Korea Research Institute of Standards and Science, Daejeon, 305-340, Korea*<sup>2</sup>*Interdisciplinary School of Green Energy and Low Dimensional Carbon Materials Center,**Ulsan National Institute of Science and Technology (UNIST), Ulsan 689-798, Korea*<sup>3</sup>*Insilicotech Co., Ltd., C602, Korea Bio Park, 694-1, Sampyeong-dong, Seongnam-si, Gyeonggi-do 463-400, Korea*

(Received 23 October 2010; revised manuscript received 22 March 2012; published 4 April 2012)

The hydrogen spillover mechanism has been discussed in the field of hydrogen storage and is believed to have particular advantage over the storage as metal or chemical hydrides. We investigate conditions for practicality realizing the hydrogen spillover mechanism onto carbon surfaces, using first-principles methods. Our results show that contrary to common belief, types of hydrogenation configurations of graphene (the aggregated all-paired configurations) can satisfy the thermodynamic requirement for room-temperature hydrogen storage. However, the peculiarity of the paired adsorption modes gives rise to a large kinetic barrier against hydrogen migration and desorption. It means that an extremely high pressure is required to induce the migration-derived hydrogenation. However, if mobile catalytic particles are present inside the graphitic interstitials, hydrogen migration channels can open and the spillover phenomena can be realized. We suggest a molecular model for such a mobile catalyst which can exchange hydrogen atoms with the wall of graphene.

DOI: [10.1103/PhysRevB.85.155408](https://doi.org/10.1103/PhysRevB.85.155408)

PACS number(s): 68.43.Bc, 88.30.R–

## I. INTRODUCTION

The hydrogenation states of graphene or graphitic material have long been studied from various viewpoints.<sup>1,2</sup> The predominance of molecular hydrogen in interstellar media has been explained by the interplay between chemisorption and physisorption modes of hydrogen atoms onto graphene.<sup>3,4</sup> Hydrogen-induced defects in graphene have been investigated with respect to metal-free magnetism and band-gap engineering.<sup>5,6</sup> Even greater interest comes from the field of hydrogen storage. Because the physisorption of molecular hydrogen onto a graphitic surface is very weak, a storage system based on such a mechanism can operate only under cryogenic conditions.<sup>7</sup> On the other hand, for room-temperature storage, the utility of the hydrogen chemisorption onto graphene has been examined but is still debated. Recent theoretical studies have shown that chemisorption states onto graphene can be exothermically stabilized through clusterization of hydrogen adsorbates in chairlike conformation.<sup>8–10</sup> In parallel, researchers have discussed the hydrogen spillover phenomena in which hydrogen atoms are claimed to be stored as chemisorption states after migration from catalytic metal sites.<sup>11–14</sup>

### A. Spillover mechanism

The essence of the hydrogen spillover, in the context of hydrogen storage, consists of three elementary steps. The first is the activation or dissociation of H<sub>2</sub> molecules on catalytic metal sites. The second is a transition of atomic hydrogen across the metal-receptor interface. The third is the migration of atomic hydrogen throughout the receptor surface. These processes are shown as 1,2; 3,4; and 5,6, respectively, in Fig. 1(a). Here, the receptor [R in Fig. 1(a)] is considered inert toward the unactivated H<sub>2</sub> gas and thus takes in only the activated atomic hydrogens that migrated from the catalyst [C in Fig. 1(a)].<sup>15</sup> It is thought that the first process [noted 1 and 2 in Fig. 1(a)] is well activated at ambient

conditions. The more fundamental issue concerns migration through the receptor surface, as described by processes 5 and 6 in Fig. 1(a). As is the cases in adsorption isotherms for surfaces, at a given pressure and temperature, the stored phase on the receptor surface should be equilibrated with the H<sub>2</sub> gas through the whole spillover process. This means that the receptor surface should simultaneously provide an appropriate thermodynamic stability (binding energy) and good kinetic mobility (migration).

### B. The carbon surface as a receptor

The spillover phenomena of activated species from catalytic metal sites onto adjacent inert surfaces have been observed for types of receptors.<sup>16</sup> Nevertheless, in the field of hydrogen storage, particular interest has been focused on carbon surfaces. Since porous carbon structures with large surface areas have commonly been synthesized, the feasibility of hydrogen spillover onto a carbon surface implies a potential breakthrough in room-temperature storage. However, although numerous researchers implicitly assumed the storage into carbon material through the spillover process, its microscopic details have not been validated theoretically or experimentally. In this study, we consider whether a pure *sp*<sup>2</sup> carbon surface can simultaneously provide thermodynamic stability and kinetic mobility of stored hydrogen.

## II. COMPUTATION METHOD

We performed density-functional theory calculations using the Vienna Ab Initio Simulation package (VASP) and the Cambridge Serial Total Energy package (CASTEP).<sup>17–20</sup> The plane-wave basis set was expanded with the energy cutoff of 400 eV. The Perdew-Burke-Ernzerhof (PBE)-type gradient-corrected density functional was employed for the exchange-correlation potential.<sup>21</sup> The potentials from ion cores were described with the projector augmented wave (PAW) method and the ultrasoft pseudopotentials for the work of VASP

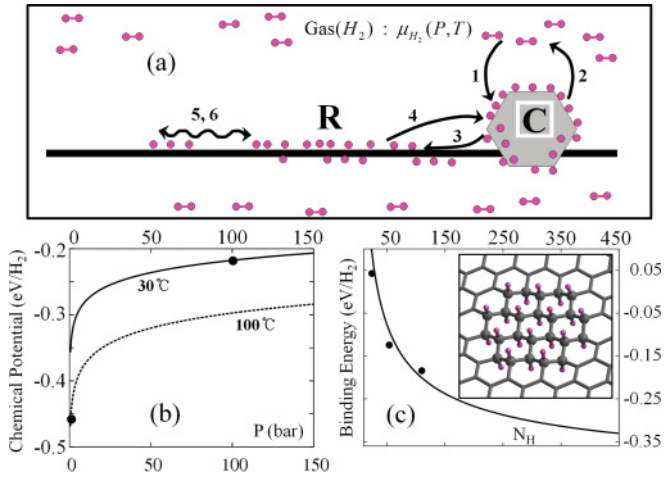


FIG. 1. (Color online) (a) Schematic description of the hydrogen spillover process. C and R indicate the catalytic metal island and the receptor surface, respectively. (b) Chemical potential (eV) of  $H_2$  gas with respect to the zero-temperature static energy of the  $H_2$  molecule. (c) Static chemisorption binding energy (eV) per  $H_2$  onto graphene. The energy reference is with respect to pristine graphene and an isolated  $H_2$  molecule. The inset shows the chemisorption geometry of 24 hydrogen atoms in the chairlike aggregated configuration. Small (pink) balls represent hydrogen atoms. The carbon atoms to which hydrogen atoms are attached are described with larger gray balls. Other parts of the graphene are denoted only with the wire frame.

and CASTEP, respectively.<sup>22,23</sup> Transition states were searched by the linear and quadratic synchronous transit method (LST/QST) implemented in CASTEP.<sup>24</sup> Our model geometries consist of a single layer of graphene with various hydrogen adatoms. We used a  $(9 \times 9)$  supercell with periodic boundary conditions, and the  $\Gamma$  point was selected in the Brillouin zone sampling. The in-plane lattice length was optimized for each case of hydrogen adsorptions. Along the perpendicular direction, a large vacuum region ( $\sim 10$  Å) was placed to simulate the isolated graphene.

### III. RESULTS AND DISCUSSION

#### A. Thermodynamic requirement

In Figs. 1(b) and 1(c), we show the stability of the hydrogen chemisorption state of graphene in comparison with the chemical potential of  $H_2$  gas. The entropy of the adsorbed phase is negligible compared to the gas phase. Thus, the adsorption binding energy must have a magnitude similar to the chemical potential of  $H_2$  gas in order to achieve a Gibbs equilibrium. For example, if a storage system is designed to be charged at 100 bar and  $30^\circ\text{C}$  and discharged at 1 bar and  $100^\circ\text{C}$ , as denoted with two solid circles in Fig. 1(b), the adsorption binding strength should be about  $0.3$  eV/ $H_2$ . In this regard, recent theoretical studies are significantly noteworthy: when the hydrogen adatoms chemisorb on both sides of graphene in a chairlike form and thereby render the corresponding carbon atoms in  $sp^3$ -hybridized state, the chemisorption states become substantially stabilized.<sup>8–10</sup>

To obtain a quantitative prediction, we placed three different numbers of hydrogen adsorbates ( $N_H = 24, 54, 110$ ) onto a single layer of graphene in a chairlike configuration, as shown in the inset of Fig. 1(c). The energetics can be described with two parameters: the energy gain proportional to the number of C-H bonds ( $N_H$ ), and the energy cost at the boundary between the  $sp^2$  and  $sp^3$  regions in proportion to the number of C-C bonds at the boundary ( $\sim \sqrt{N_H}$ ).<sup>8,9</sup> As a result, the static binding energy per  $H_2$  can be parameterized as  $E_b = -A + B/\sqrt{N_H} - E(H_2)$ , where  $E(H_2)$  represents static total energy of the isolated  $H_2$  molecule. The constant  $A$  is obtained from the binding energy per  $H_2$  in the completely hydrogenated graphene case ( $N_H \rightarrow \infty$ ),<sup>9</sup> and the parameter  $B$  is fitted with the cases of  $N_H = 24, 54$ , and  $110$ . As shown in Fig. 1(c), the fitted model predicts that if the size of hydrogenated  $sp^3$  domain is bigger than that of  $N_H \sim 200$ , the hydrogen chemisorption binding energy becomes similar to the chemical potential of  $H_2$  gas [see Fig. 1(b)], thereby satisfying the thermodynamic requirement for room-temperature operations.

#### B. Effect of pairing and clustering

To achieve a clearer understanding of the aforementioned energetics, we considered configurations of hydrogen dimers on a graphene surface. Figures 2(a)–2(c) show the optimized geometries of the hydrogen adsorbates in the ortho-, meta-, and para-dimer configurations, respectively. In the  $AA2\sqrt{3}$  configuration as shown in Fig. 2(d), two hydrogen atoms occupy the same sublattice (A), separated by  $2\sqrt{3}$  times the C-C bond length. The uu in the parentheses indicates that both hydrogen atoms are on the up side of the graphene. The geometries shown in Figs. 2(e)–2(h) are the same cases as Figs. 2(a)–2(d), respectively, with one hydrogen atom on the opposite side of the graphene.

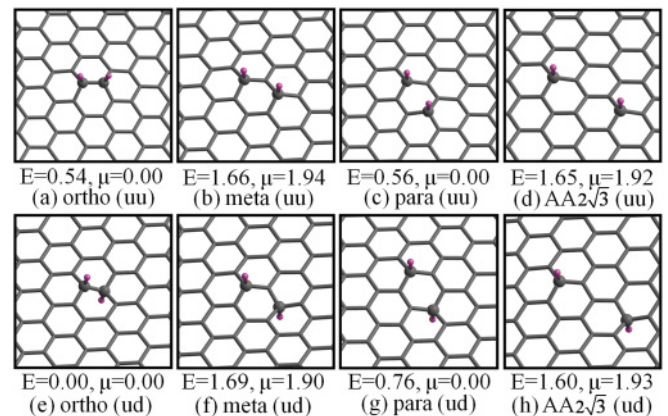


FIG. 2. (Color online) Models for the chemisorbed hydrogen dimers on the graphene plane. The (uu) in (a)–(d) indicate that two hydrogen adatoms are on the up side of the plane. The same dimer configurations with one hydrogen adatom on the up and the other one on the down side, as depicted with (ud), are shown in (e)–(h). The total energy differences (eV) are given with respect to the case of ortho(ud). Atomic symbols follow the same convention as in Fig. 1.

We note that two mechanisms contribute to the overall energetics: one is the dimerization effect in the hyperconjugated  $\pi$  network, and the other is the strain effect in the carbon framework. In the cases of ortho- and para-dimers, two hydrogen adatoms remove two  $p_z$  electrons from the  $\pi$  network: one from each sublattice (A,B) of the graphene bipartite system. Thus the remaining  $\pi$  electrons are well paired, resulting in lower energy. On the contrary, in the cases of the meta-dimer and  $AA2\sqrt{3}$ , the two hydrogen atoms adsorb onto one sublattice (A), leading to a magnetized electronic ground state. The net spin ( $\mu$ ) calculated with the spin-polarized density functionals are shown in Fig. 2. For a finite size graphene fragment, these types of magnetism have been discussed with the Hubbard model and summarized by the Lieb's counting rule, which is also consistent with the Kekulé diagram.<sup>25,26</sup>

An additional energy component comes from the strain in the C-C bond. The carbon atoms to which hydrogen adatoms are bonded have  $sp^3$  states, thereby inducing strain in neighboring C-C bonds. The energy difference between ortho(uu) and ortho(ud) suggests the strain effect: two C atoms in the ortho(ud) configuration better fit the carbon  $sp^3$  bonds and are less strained. When a large number of hydrogen adatoms adsorbates accumulate on the graphene surface, they favor the electronically paired configurations. Also, they are likely to aggregate in a less-strained configuration. The chairlike configurations with adatoms aggregated in a circular pattern maximize the area of the unstrained domain and become the least strained.

### C. Unpaired dimers are vulnerable to desorption

When hydrogen adatoms are not paired, they are prone to desorption. Figures 3(a)–3(c) show the energy barrier along the desorption of  $H_2$  from two unpaired configurations [Figs. 3(a) and 3(b)] and one paired configuration [Fig. 3(c)]. This shows that the unpaired parts of the hydrogen adatoms are likely to desorb upon heat treatment, leaving behind the paired hydrogenated domain. For an explicit comparison, the migration barrier of one unpaired hydrogen atom is shown in Fig. 3(d). This shows that the unpaired hydrogen atoms are likely to desorb into gaseous  $H_2$  rather than migrate onto the graphene surface forming paired domains. The previous experiment showed that some parts of the hydrogen adatoms desorb easily by annealing at room temperature, while some remaining parts can robustly survive a high-temperature heating.<sup>2</sup> From these results we understand that the observed stable clusters of hydrogen adatoms probably had features of the paired configurations.

### D. Stability against hydrogen migration

We now show that the edge of the paired chairlike hydrogenated domain is particularly inert against hydrogen migration. As a model system, we considered the geometries of the chairlike configuration of 24 hydrogen adatoms as shown in Fig. 4(a). The one-hydrogen-migrated and two-hydrogen-migrated configurations [Figs. 4(b) and 4(c)] have substantially higher energy than the all-paired aggregated chairlike configuration [Fig. 4(a)]. For the case shown in

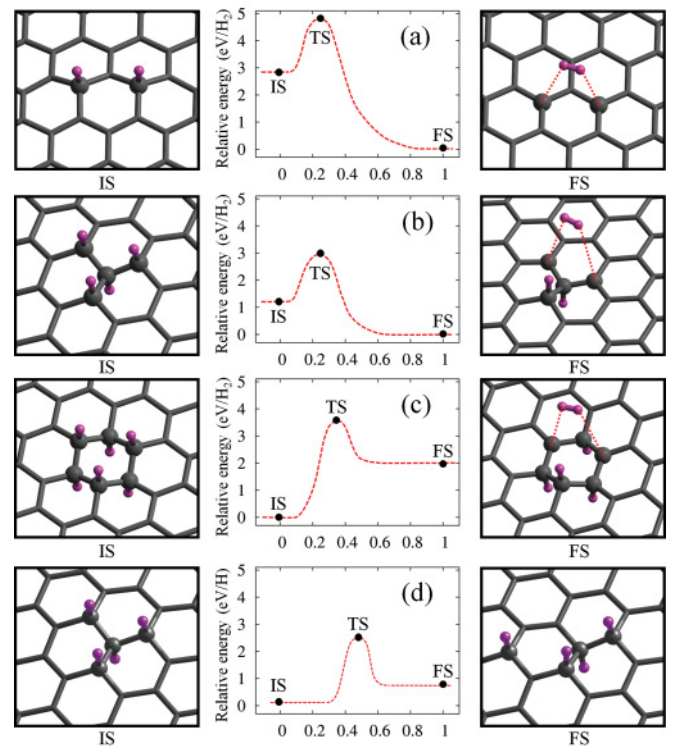


FIG. 3. (Color online) Energy barriers along the desorption of  $H_2$  from (a) the meta-dimer configuration, (b) the unpaired chairlike four hydrogen adatoms, and (c) the paired chairlike six hydrogen adatoms configuration. (d) The migration barrier for one unpaired hydrogen atom from the IS of (b). IS, FS, and TS represent the initial state, final state, and transition state, respectively. The geometries of each IS and FS are shown in the left and right panels of each energy curve. The dashed curves connecting IS, FS, and TS are only for guide. Atomic symbols follow the same convention used in Fig. 1.

Fig. 4(b), the carbon atom from which the hydrogen migrated has an unpaired  $p_z$  electron and thus becomes electronically very unstable.

In the two-hydrogen-migrated case [Fig. 4(c)], the two  $p_z$  electrons at the two hydrogen-removed carbon sites form a localized  $\pi$  bonding state. In terms of the electronic structure, this structure can be more stable than the one-hydrogen-migrated case. Nevertheless, the localized  $\pi$  state induces an energy cost in the Coulomb energy, thereby rendering the two-hydrogen-migrated case more unstable than the case of Fig. 4(a).<sup>27</sup> We also observe that the migrated two-hydrogen atoms constitute the para(ud) geometry. The energy difference between the ortho(ud) and para(ud) configurations, as shown in Fig. 2, applies to this case as well. The same cases with 54 hydrogen adatoms are shown in Figs. 4(d)–4(f). The energy barriers along the aforementioned migrations were also calculated, as shown in Fig. 5. The figure confirms again that the edge of the paired chairlike hydrogenated domain is highly inert against the migration. This suggests that an effective exposure of both surfaces of graphene can lead to stable hydrogenated domains, as observed in recent experiments.<sup>29</sup> This type of all-paired hydrogenation is useful for band-gap engineering of graphene.



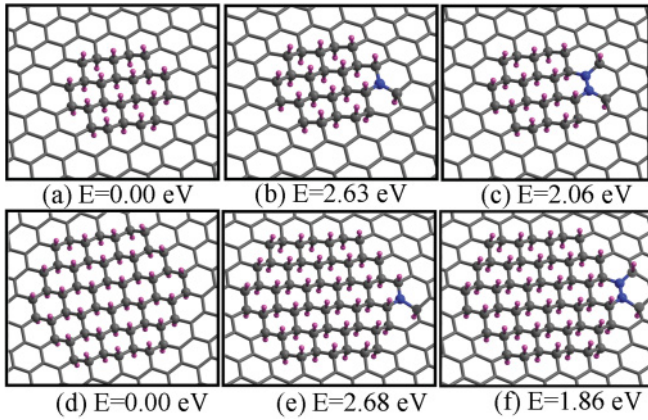


FIG. 4. (Color online) The optimized geometries of 24 hydrogen adatoms in (a) all-paired aggregated chairlike configuration, (b) one-hydrogen-migrated, and (c) two-hydrogen-migrated configurations, respectively. (d), (e), and (f) correspond to the same configurations of 54 hydrogen adatoms, respectively. The energies denoted in (b) and (c) are with respect to that of (a), and those shown in (e) and (f) are with respect to that of (d). Atomic symbols follow the same convention used in Fig. 1. In (b), (c), (e), and (f), the carbon atoms from which hydrogen atoms migrated are emphasized with a different gray scale (blue).

### E. Our main result

A previous experiment suggested that the observed hydrogen desorption rate at 217 °C corresponds to the desorption barrier of 1.38 eV per  $\text{H}_2$ .<sup>2</sup> Another report suggested that a heat treatment at about 450 °C (24 hours in Ar atmosphere) is required for cleaning the hydrogenated graphene.<sup>1</sup> In this work, we showed that the migration barrier from the edge of the chairlike hydrogenated domain is about 2~3 times higher than the desorption barrier from the unpaired configurations [Figs. 3(a) and 3(b)]. If we are considering simple first-order Arrhenius-type diffusion [ $\nu = \nu_0 \exp(-\Delta E/kT)$ ], this suggests that a measurable rate of hydrogen migration requires heating at about several hundred degrees Celsius. However, such heating would linearly lower the chemical potential of gas-phase hydrogen [ $\mu_{\text{H}_2}(P, T)$ ].<sup>28</sup> The desorption channel of hydrogen, as denoted by process 2 in Fig. 1(a), would

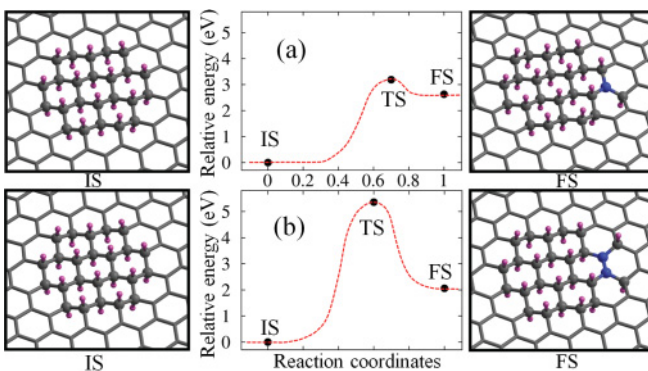


FIG. 5. (Color online) The energy barrier along the migration of (a) one and (b) two hydrogen adatoms from the edge of a paired chairlike hydrogenated domain. The atomic symbols and abbreviations follow the same convention used in Fig. 4.

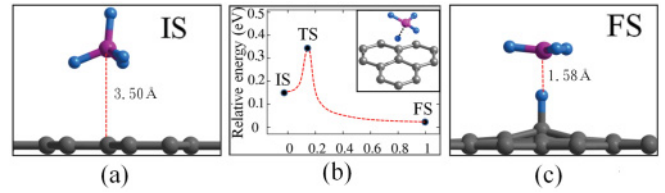


FIG. 6. (Color online) Hydrogen exchange between  $\text{BH}_4^-$  and graphene. (a) Optimized geometry of  $\text{BH}_4^-$  anion on graphene. (b) The energy barrier along the hydrogen transfer from  $\text{BH}_4^-$  to graphene. (c) The optimized geometry after one hydrogen atom transferred onto graphene. The abbreviation IS, TS, FS indicate initial states, transition state, and final state, respectively. Inset of (b) shows the TS.

be greatly enhanced at such high temperature, leading to discharge of stored hydrogen. Our results tell that the pure  $sp^2$  carbon surface cannot be a receptor for spillover hydrogen.

However, if some external agency can help the hydrogen migration, the concept of spillover can be practically utilized for hydrogen storage on the carbon surface. Here we provide one example. Figure 6 shows the adsorption of  $\text{BH}_4^-$  molecular anions on graphene. The energy barrier for the diffusion of  $\text{BH}_4^-$  on the carbon surface is almost negligible (not shown). In addition, the dispatch of one hydrogen atom from  $\text{BH}_4^-$  onto the graphene surface involves only a small energy barrier of about 0.23 eV. This indicates that if this sort of molecular species encapsulates inside the graphitic galleries, it can provide a mobile catalysis which can exchange hydrogen atoms with the carbon surface and carry hydrogen atoms deep inside the carbon surface.

## IV. CONCLUSION

In summary, we used the density-functional theory methods to investigate the thermodynamic stability and kinetic features of hydrogen chemisorption states of graphene. The particular geometry of the chairlike all-paired configuration of hydrogen adatoms can satisfy the thermodynamic requirement for room-temperature hydrogen storage. However, such configurations have a large barrier against hydrogen migration along the graphenelike carbon surface. Activation of a migration channel requires high-temperature heating, and thus the thermodynamic stability and kinetic mobility cannot be obtained simultaneously. In order to realize the spillover-based storage mechanism, the credibility of hydrogen migration along the surface of the receptor should be established, which cannot be obtained with pure  $sp^2$ -bonded carbon structures. We, however, suggest that the concept of hydrogen spillover can be utilized with the carbon surface if some moving catalysis can be introduced. As an example, we showed the hydrogen exchange between  $\text{BH}_4^-$  and graphene.

## ACKNOWLEDGMENT

This research was performed for the Hydrogen Energy R&D Center, a 21st Century Frontier R&D Program, funded by the Ministry of Science and Technology of Korea.

\*Corresponding author: dhjung@insilicotech.co.kr

†Corresponding author: noejung@unist.ac.kr

- <sup>1</sup>D. C. Elias, R. R. Nair, T. M. G. Mohiuddin, S. V. Morozov, P. Blake, M. P. Halsall, A. C. Ferrari, D. W. Boukhvalov, M. I. Katsnelson, A. K. Geim, and K. S. Novoselov, *Science* **323**, 610 (2009).
- <sup>2</sup>L. Hornekær, Ž. Šljivančanin, W. Xu, R. Otero, E. Rauls, I. Stensgaard, E. Lægsgaard, B. Hammer, and F. Besenbacher, *Phys. Rev. Lett.* **96**, 156104 (2006).
- <sup>3</sup>M. Bonfanti, R. Martinazzo, G. F. Tantardini, and A. Pointi, *J. Phys. Chem. C* **111**, 5825 (2007).
- <sup>4</sup>X. Sha, B. Jackson, and D. Lemoine, *J. Chem. Phys.* **116**, 7158 (2002).
- <sup>5</sup>O. V. Yazyev, *Rep. Prog. Phys.* **73**, 056501 (2010).
- <sup>6</sup>H. Xiang, E. Kan, S.-H. Wei, M.-H. Whangbo, and J. Yang, *Nano Lett.* **9**, 4025 (2009).
- <sup>7</sup>S. K. Bhatia and A. L. Myers, *Langmuir* **22**, 1688 (2006).
- <sup>8</sup>Y. Lin, F. Ding, and B. I. Yakobson, *Phys. Rev. B* **78**, 041402(R) (2008).
- <sup>9</sup>J. O. Sofo, A. S. Chaudhari, and G. D. Barber, *Phys. Rev. B* **75**, 153401 (2007).
- <sup>10</sup>D. Stojkovic, P. Zhang, P. E. Lammert, and V. H. Crespi, *Phys. Rev. B* **68**, 195406 (2003).
- <sup>11</sup>Y. Li and R. T. Yang, *J. Am. Chem. Soc.* **128**, 8136 (2006).
- <sup>12</sup>C. S. Tsao, Y.-R. Tzeng, M.-S. Yu, C.-Y. Wang, H.-H. Tseng, T.-Y. Chung, H.-C. Wu, T. Yamamoto, K. Kaneko, and S.-H. Chen, *J. Phys. Chem. Lett.* **1**, 1060 (2010).
- <sup>13</sup>L. Chen, A. C. Cooper, G. P. Pez, and H. Cheng, *J. Phys. Chem. C* **111**, 18995 (2007).
- <sup>14</sup>G. M. Psofogiannakis and G. E. Froudakis, *J. Am. Chem. Soc.* **131**, 15133 (2009).
- <sup>15</sup>Experiments have been performed with porous carbon samples with embedded metal particles. It is naturally considered that both surfaces of  $sp^2$  carbons (up or down) are available for migration of hydrogen atoms from metal surfaces.
- <sup>16</sup>H. L. Tierney, A. E. Baber, J. R. Kitchin, and E. C. H. Sykes, *Phys. Rev. Lett.* **103**, 246102 (2009).
- <sup>17</sup>P. Hohenberg and W. Kohn, *Phys. Rev.* **136**, B864 (1964).
- <sup>18</sup>W. Kohn and L. J. Sham, *Phys. Rev.* **140**, A1133 (1965).
- <sup>19</sup>G. Kresse and J. Furthmüller, *Phys. Rev. B* **54**, 11169 (1996); *Comput. Mater. Sci.* **6**, 15 (1996).
- <sup>20</sup>S. J. Clark, M. D. Segall, C. J. Pickard, P. J. Hasnip, M. I. J. Probert, K. Refson, and M. C. Payne, *Z. Kristallogr.* **220**, 567 (2005).
- <sup>21</sup>J. P. Perdew, K. Burke, and M. Ernzerhof, *Phys. Rev. Lett.* **77**, 3865 (1996).
- <sup>22</sup>D. Vanderbilt, *Phys. Rev. B* **41**, 7892 (1990).
- <sup>23</sup>G. Kresse and D. Joubert, *Phys. Rev. B* **59**, 1758 (1999).
- <sup>24</sup>T. A. Halgren and W. N. Lipscomb, *Chem. Phys. Lett.* **49**, 225 (1977).
- <sup>25</sup>E. H. Lieb, *Phys. Rev. Lett.* **62**, 1201 (1989).
- <sup>26</sup>J. Cho, S. Lim, J. Cha, and N. Park, *Carbon* **49**, 2665 (2011).
- <sup>27</sup>For the case of the all-paired chairlike configurations, the  $\pi$  electron states are decently delocalized over the  $sp^2$ -bonded carbon atoms.
- <sup>28</sup>For example, at about 500 °C and 1 atm, the chemical potential of hydrogen gas approaches  $-1$  eV [see the plot in Fig. 1(b)]. Thus, at such high temperature, the adsorbed phases on the metal catalyst or receptor surface become unstable in comparison with the hydrogen gas phase.
- <sup>29</sup>R. Balog, B. Jorgensen, L. Nilsson, M. Andersen, E. Rienks, M. Bianchi, M. Fanetti, E. Lægsgaard, A. Baraldi, S. Lizzit, Z. Slijivančanin, F. Besenbacher, B. Hammer, T. G. Pedersen, P. Hofmann, and L. Hornekær, *Nature Mater.* **9**, 315 (2010).